NASA TECHNICAL NOTE

NASA TN D-1896

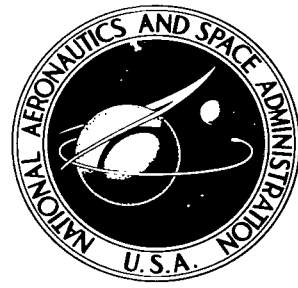

NASA TN D-1896

THERMAL PERFORMANCE AND RADIO-FREQUENCY TRANSMISSIVITY OF SEVERAL ABLATION MATERIALS

by Marvin B. Dow, Claud M. Pittman, and William F. Croswell

Langley Research Center
Langley Station, Hampton, Va.

NATIONAL AERONAUTICS AND SPACE ADMINISTRATION • WASHINGTON, D. C. • NOVEMBER 1964

THERMAL PERFORMANCE AND RADIO-FREQUENCY TRANSMISSIVITY OF SEVERAL ABLATION MATERIALS

By Marvin B. Dow, Claud M. Pittman, and William F. Croswell

Langley Research Center
Langley Station, Hampton, Va.

NATIONAL AERONAUTICS AND SPACE ADMINISTRATION

For sale by the Office of Technical Services, Department of Commerce, Washington, D.C. 20230 -- Price $1.00

THERMAL PERFORMANCE AND RADIO-FREQUENCY TRANSMISSIVITY OF SEVERAL ABLATION MATERIALS

By Marvin B. Dow, Claud M. Pittman,
and William F. Croswell
Langley Research Center

SUMMARY

An investigation was made of the thermal performance of ablation materials and of the attenuation of radio signals by degraded ablation materials. Nine cone-shaped models, consisting of a truncated magnesium-alloy shell and a contoured plastic nose cap with various heat-shielding materials bonded to the magnesium shell, were tested in the 2500-kilowatt arc jet at the Langley Research Center. Temperature measurements at several locations on the interior of the magnesium shells and measurements of radio-frequency attenuation due to thermal degradation of the protective materials were made. The relative thermal effectiveness of each material in the arc-jet environment was calculated from data obtained during testing. Photographs are presented which show the effects of the test environment on the various heat-shielding materials and on ring antenna windows of Teflon inserted into some of the test materials. A comparison between calculated and experimentally measured temperatures on the interior of the magnesium shell was made for two of the heat-shielding materials.

INTRODUCTION

The metal telemetry antennas of certain high-velocity reentry vehicles must be protected from the severe heating conditions encountered during reentry. In order to permit data telemetry to ground stations after severe heating ceases, the thermal protection material used over the telemetry antennas must not seriously attenuate radio transmission after thermal degradation. Some information is available on the thermal protection characteristics of many ablation materials. However, little information is available on their radio-transmission-attenuation characteristics after thermal degradation. Therefore, an experimental investigation was conducted to obtain data on the attenuation characteristics after thermal degradation of various ablation materials bonded to a metal antenna and also to obtain data on the relative effectiveness of the various thermal protection materials in limiting the temperature rise of the metal structure and antenna. The use of antenna windows in thermal protection materials having unacceptable attenuation levels was also investigated. The criteria used in evaluation of radio transmission attenuation were that there be no more than a 2-decibel attenuation at frequencies from 200 to 250 Mc, the frequency range often used in reentry-vehicle telemetry systems.

This paper presents the results of tests on nine cone-shaped models, consisting of a truncated magnesium-alloy shell and a contoured plastic nose cap with various heat-shielding materials bonded to the magnesium shells, which were exposed to convective heating in the 2500-kilowatt arc jet at the Langley Research Center. Supplemental apparatus was used for attenuation measurements. In addition, a comparison between calculated and experimentally measured temperatures on the interior of the magnesium shell was made for two of the heat-shielding materials.

SYMBOLS

The units used for the physical quantities defined in this section are given both in the U.S. customary units and in the International System of Units, SI. (See ref. 1.) An appendix is included for the purpose of explaining the relationships between these two systems of units.

E	thermal effectiveness, Btu/lb or J/kg
l	length of afterbody, in. or m
q	cold-wall heating rate, Btu/(sq ft)(sec) or W/m^2
q_x	cold-wall heating rate at distance x
$q_{x=0}$	cold-wall heating rate at $x = 0$
t	time, sec
w	weight distribution of ablation material, lb/sq ft or kg/m^2
x	distance from junction of nose cap and 9° conical afterbody, in. or m

TEST MODELS

The pertinent dimensions and construction details of the models used in ground tests of afterbody thermal protection materials are shown in figure 1. The models were fabricated as cones to provide realistic conditions in regards to severe differential expansion between the protective material and the metal substructure resulting from the model shape and the dissimilar thermal expansion rates of the materials. The conical portion of the models consisted of a ring-stiffened shell of HK31A magnesium alloy, 1/16 inch (1.59 mm) thick; one end ring was threaded internally for attachment of the nose cap. The shell was separated into two sections by a phenolic-nylon ring. The large end of the shell was stiffened by a plastic ring which also provided a means of attaching the specimen to the steel cover plate and thus to the test fixture. The plastic nose cap was machined from phenolic asbestos and was screwed into the threads on the end ring of the shell. The nose cap forced the test material to expand

longitudinally in the direction of the large end of the cone. The graphite cover was loose fitting and served as a fairing between the model and the test fixture and also protected the rear of the model from heating. Thermocouples were attached to the magnesium-alloy shell, the back of the nose cap, and the steel cover plate, as shown in figure 1.

The test material was attached to the exterior of the magnesium shell. All materials were 1/4 inch (0.635 cm) thick; thus, the weight distributions, pounds per square foot (kilograms per square meter), of the different materials vary as the densities.

It was anticipated that the char or debris layer which develops on certain shielding materials during heating would cause radio attenuation. For this reason, it was decided to investigate the use of an antenna window in conjunction with the char- or debris-forming materials. The superior heat-shielding characteristics of these materials could be utilized by such an arrangement. Therefore, a second type of model was constructed which had an antenna window consisting of a Teflon ring adhesively bonded to the phenolic-nylon ring separating the magnesium-alloy shell. (See fig. 1.) The Teflon ring, which was the same thickness as the test material, separated the test material so that it covered only the metal portions of the cone. It should be noted that for use as antenna windows, there are materials more suitable than Teflon, such as ceramics, reinforced Teflon, or preferentially oriented nylon fibers. The inability to duplicate flight velocity, heating rate, and enthalpy in ground tests did not warrant an extensive investigation of various types of antenna-window materials for possible use on reentry vehicles.

Typical models constructed with and without antenna windows are shown in figure 2. Table I is a summary of the materials tested, their composition, and the method of bonding to the metal cone.

TEST APPARATUS AND CONDITIONS

The models were tested in the 2500-kilowatt arc jet at the Langley Research Center (LRC) with air as the test medium. The details of the construction and operation of this facility are presented in reference 2. This arc-jet facility is characterized by subsonic flow and an enthalpy of approximately 3,000 Btu/lb (6.97×10^6 J/kg).

Both the stream velocity and enthalpy available from this facility are substantially lower than those which would be encountered by a typical reentry vehicle. The nature of the ground tests, however, required test models of the size used, and the 2500-kilowatt arc jet at LRC was the only available facility with the capability of testing large models. For these tests a nozzle 6 inches (15.2 cm) in diameter was used, and the mass flow of air from the nozzle was 0.35 lb/sec (0.1585 kg/s).

The "cold-wall" heating-rate distribution on the afterbody of the test models is shown in figure 3. The heating on the model was assumed to be

convective only, inasmuch as the negligible optical thickness of the gas layer and previous radiant-heating measurements preclude the presence of significant radiant heating. The model heat-transfer rates were determined by use of a metal calorimeter of the same size and shape as the test models.

The test setup shown in figure 4 was used to determine the amount of radio attenuation caused by thermal degradation of the various test materials and, simultaneously, to determine the relative performance of the test materials as afterbody thermal protection in the arc-jet environment.

An 11-element yagi transmitting antenna was located in a wooden box about 2 feet (0.61 m) square and 15 feet (4.57 m) long. The opening in the box was located about 2 feet (0.61 m) from the specimen (fig. 4) and the end of the antenna, about 14 feet (4.27 m) from the arc-jet nozzle to provide a far-field pattern. The transmitting antenna was connected by a coaxial cable to a calibrated signal source operating at 950 Mc. The signal source was operated at a higher frequency than typical reentry-vehicle telemetry frequencies to minimize the scattering effects from objects in the test area which were immovable and necessary in arc-jet operation. The model as shown in figure 4 was the receiving antenna (a common practice because of space considerations which, in this case, also minimized thermocouple interference) and was connected by a coaxial cable to a receiver. The coaxial cable was carried through the model support to the inside of the model where the shield of the coaxial cable was connected to one section of the magnesium-alloy shell, and the center conductor of the cable was connected to the second shell section. The automatic gain control (AGC) of the receiver was connected to an oscillograph. In order to minimize reflections from the walls, pipes, and other objects in the test area, absorber material was used to line the box supporting the transmitting antenna, and screens of absorber material were placed all around the arc-jet facility. In addition, the transmitter and receiver were located away from the immediate test area in the locations that minimized direct coupling from transmitter to receiver.

TEST PROCEDURES

Before each test, pattern and impedance measurements were performed on each model to determine its performance as an antenna. Because of the large number of thermocouple lead wires, it was difficult to control exactly the impedance and pattern from model to model, but the nature of the tests made this consideration a secondary one. In all instances, the voltage standing-wave ratio (VSWR) of the model was less than 3 to 1 at 950 Mc, and the antenna patterns were roughly similar to a dipole pattern. The characteristics were considered acceptable.

The primary purpose of the measurements of radio attenuation was to determine the amount of attenuation that occurred because of thermal degradation of the test material. This measurement was obtained by a simple comparison of signal level before and immediately after heating of the model in the arc jet. Before testing, the model was placed in the test position and the received AGC output was calibrated. The model was then removed from the test position, the

arc jet was started, and the model was reinserted for testing. The received signal strength was recorded throughout the entire test and for several minutes after the test. However, for reasons discussed in a later portion of the paper, it was not possible to obtain valid attenuation measurements during actual arc-jet operation.

The procedure followed for the thermal tests, conducted simultaneously with the radio-attenuation measurements, was to start the arc jet, establish the desired operating conditions, and then insert the model into the test stream. The models remained in the test stream until a temperature of approximately 500° F (533° K) was reached on the magnesium-alloy shell or until visual observation of the specimen indicated that failure was imminent.

The upper limit of approximately 500° F (533° K) was established by the following two considerations. First, the adhesive bonding material used to attach some test materials begins to lose strength rapidly at temperatures in excess of 500° F (533° K). Second, the magnesium alloy used in fabricating the model shells contained thorium, which is radioactive; therefore, extreme caution was exercised to insure that the shell did not ignite.

RESULTS AND DISCUSSION

The test results are presented in table II and in figures 5 and 6. The radio attenuation due to thermal degradation, the relative thermal effectiveness of each test material, and the reason for the cessation of the test if for a reason other than the allowable temperature on the magnesium-alloy shell are given in table II. The temperature histories of thermocouples attached to the models (fig. 1) are shown in figure 5. Photographs of the models after testing and a section of each model are shown in figure 6.

Appearance of Tested Models

Examination of the photographs of figure 6 shows that the various test materials differed markedly in appearance after exposure to the arc-jet stream. It should be remembered that all test materials were of equal thickness. There is a substantial difference in the thickness of the various materials remaining after test exposure.

The Teflon model (fig. 6(a)) shows a large loss of thickness in the area immediately downstream of the nose cap. Teflon is commonly classified as a subliming material and therefore leaves no residue when it ablates. The discoloration of the Teflon visible in figure 6(a) was probably caused by the ablation products from the nose cap. No defects in the bond between the Teflon and the magnesium-alloy shell were noted on the complete model after testing. When the model was sectioned, however, the residual stresses in the Teflon and inadequate bonding caused separation of the Teflon from the magnesium-alloy shell, as shown in figure 6(a).

The ablation material on the Avcoat II model (fig. 6(b)) was almost completely consumed on all areas of the model, particularly in the region immediately downstream of the nose cap. The residue remaining after the ablation of Avcoat II resembled soot in color and texture. It is probable that a higher velocity stream than that used for testing would have removed this residue during the ablation process. The Avcoat II model shown in figure 6(c) had a Teflon ring antenna window. Examination of this figure shows that the Teflon receded at a slower rate than did the Avcoat II material, except for the region immediately downstream of the Teflon ring antenna window. However, the mass-loss rate was higher with Teflon because of its higher specific gravity. (See table I.) The flow disturbance caused by the protruding Teflon ring antenna window was probably responsible for the lower recession rate of the Avcoat II immediately downstream of the window.

The RTV-88 model (fig. 6(d)) exhibited pronounced swelling and buckling of the highly heated material on the surface of the cone. Inasmuch as this weak surface residue was observed sliding downstream in the low-velocity test stream, there is an indication that higher velocity flows might have completely removed this material. Examination of the complete model in figure 6(d) also shows fissures in the material beneath the residue layer. As can be seen in the section photograph, these fissures did not extend to the magnesium shell. Because of a mechanical failure on the arc jet, the test of the RTV-88 model was not of sufficient duration to produce a 500° F (533° K) temperature on the magnesium shell.

The models of phenolic nylon and phenolic nylon with a Teflon ring antenna are shown after testing in figures 6(e) and 6(f), respectively. The surface of these models shows the carbonaceous char layer formed during the ablation of this type of material. The variation in the depth of the char layer is evident in the section views of the specimens. The section view of figure 6(e) shows that the phenolic-nylon material in the region immediately downstream of the nose cap was pyrolyzed to the full depth of the material and that the charred residue has separated from the magnesium-alloy shell. The section photograph also shows faulty bonding of the phenolic nylon to the magnesium-alloy shell, as evidenced by voids and separations at the bond line in the region downstream of the separation ring. Figure 6(f) shows the severe notch effect produced by the ablation and loss of material from the Teflon ring antenna window at a more rapid rate than the phenolic nylon. References 3, 4, and 5 indicate that this notch effect would be even more severe in the flight environment than the arc-jet environment. It was this notch effect which caused testing of the specimen to be terminated before the temperature of the magnesium-alloy shell reached 500° F (533° K). During the test it was impossible to estimate the exact depth of the notch, and for the reasons previously stated it was necessary to avoid a catastrophic failure. The section view of the model in figure 6(f) also shows separation of the test material from the magnesium-alloy shell and bond-line faults similar to those of the model shown in figure 6(e).

The cork-covered model is shown after testing in figure 6(g). The surface of this model is also characterized by a carbonaceous char layer, but the surface is much more irregular than was true of the phenolic-nylon models (fig. 6(e)). As would be expected, the char surface closely resembles wood char, and the char layer was weak and friable.

The Thermo-Lag T-500 EX167 models, one with and one without a Teflon ring antenna, are shown in figures 6(h) and 6(i), respectively. The surface of the model shown in figure 6(h) had a glassy residue layer with little loss of material thickness, except in the region immediately downstream of the nose cap. The photograph of the complete model in figure 6(h) also shows several large craters which formed in the material during the test. The craters were apparently caused by gas blowouts of pyrolized material which resulted from localized pressure increases of the gases produced by thermal degradation beneath the glassy residue layer. These craters formed during testing and, because it was impossible to estimate the depth of the craters, the test was terminated lest ignition of the magnesium-alloy shell should occur in a region removed from a thermocouple. Bond-line separation and buckling of the test material are evident in the section view of the model in figure 6(h).

Radio Attenuation

The measured levels of radio attenuation for all models tested are shown in table II. Of the various materials tested, only those models containing Teflon or Avcoat II had a radio-attenuation level of 2 decibels. The radio-attenuation level of 5 decibels measured with the RTV-88 model indicates that this material might perform satisfactorily at flight frequencies. This result follows from the fact that the attenuation at typical flight frequencies from 200 to 250 Mc should be roughly one-third the level measured at the test frequency of 950 Mc. The other test materials which formed carbonaceous char or electrically conducting debris layers on the surface due to thermal degradation had attenuation levels which varied from moderate to severe, but in all instances the level of attenuation was unacceptably high and would be at flight frequencies.

The values for attenuation shown in table II should not be regarded as standard values for these particular materials because the configuration of the models and the various sources of interference precluded this type of determination. The values shown reflect only the changes in attenuation as measured for each model in the test position before the arc jet was started and immediately after the cessation of heating with the model still in the test position.

Attempts to measure the amount of attenuation occurring in the various materials during actual heating were not successful because of severe attenuation effects from the arc-jet stream. The arc-jet stream was not pure air but included, among other contaminants, copper from the electrodes. The level of attenuation, caused by the arc-jet stream, was not constant but varied widely during the period of model exposure and also varied between tests of different models, depending on the degree of contamination in the arc-jet stream. The net effect of these variations in attenuation was to make it difficult or impossible to determine the attenuation during the thermal degradation of the test material.

There was evidence of a slight decrease in the attenuation level as the test materials cooled, but this decrease did not result in any significant reduction in the attenuation level. The models which had Teflon ring antenna windows exhibited satisfactory attenuation levels even though other areas of the model were badly charred or had heavy debris layers. This result was

anticipated since it was known that the transmission of radio frequencies through Teflon is unaffected by ablation. The thin layer of material deposited on the Teflon (which came from the nose cap and the test material upstream of the ring antenna window) did not appear to influence the transmission capability of the Teflon. The impedance and antenna pattern of each specimen that exhibited relatively low attenuation were obtained after testing and were similar to those measurements made prior to the arc-jet test.

Relative Material Effectiveness

A useful parameter for evaluating the relative thermal effectiveness of materials is defined as the total cold-wall heat input to the front surface required to produce a certain temperature rise at the back surface divided by the weight distribution of the ablation material. That is, $E = \frac{qt}{w}$.

The relative effectiveness of the various test materials calculated in this manner for magnesium-shell temperatures of 100° F (311° K), 300° F (422° K), and 500° F (533° K) are shown in table II. For these calculations, the materials were evaluated at the locations of thermocouples 2 and 5 (fig. 1), where the cold-wall heating rate of 45 Btu/(sq ft)(sec) $(51 \times 10^4 \text{ W/m}^2)$ was obtained from figure 3. The times required to produce specified temperatures on the magnesium shell were obtained from figure 5. Because of temperature gradients along the afterbody, heat was conducted toward the downstream end of the specimens. The calculations are not corrected for the conduction effect which causes an apparent increase in the material effectiveness. Those instances for which an effectiveness is not shown are due to the termination of the test before the prescribed shell temperatures were reached.

The various test materials show a wide range of values, with cork having the highest values and Teflon, the lowest values. It should be noted that the relative effectiveness is a strong function of the environment in which it is evaluated. In the arc-jet environment in which these tests were performed, the enthalpy is relatively low, and blocking of the convective-heat input by the gases transpired into the boundary layer is relatively inefficient. Therefore, materials which form a char layer and thus radiate a considerable part of the heat input show a higher effectiveness than materials which rely primarily on blocking for their effectiveness. However, in a high enthalpy flight environment, injection of the ablation products into the boundary layer is much more effective in blocking the heat input, and all the materials should show much improved effectivenesses. This improvement will probably not be the same for all materials, and therefore the relative effectiveness of the materials may be different. Also the flight environment produces much larger shear stresses, and a material such as Avcoat II, which produces a very weak char layer in the arc jet, would probably behave as a subliming material in flight.

Temperature Histories

Curves of temperature plotted against time for the thermocouples attached to each model are shown in figure 5. The vertical dashed line indicates the

time at which the arc jet was turned off. The temperature rise which occurred after this time was due to heat stored in the test material. Some thermocouples became inoperative on a few models; therefore, less than 10 temperature histories are shown for these specimens in figures 5(c), 5(d), and 5(f).

Examination of the temperature histories for thermocouple 1 in figure 5 reveals that in all cases the thick plastic nose cap effectively blocked the flow of heat from the front region of the model to the magnesium-alloy shell. The magnesium shell on all models, except the one for which the test material was Teflon, showed almost no temperature rise for the first 20 seconds of exposure. The magnesium shell of the model covered with Teflon shows an immediate temperature rise because Teflon is not opaque to radiant energy from the hot gases and from the hot outer regions of the material itself. The temperature histories for all models, except those for which the test was terminated for various reasons, show similar behavior in that the temperature of the magnesium shell is maintained at relatively low values until the test material is consumed or until the char layer reaches the magnesium. When this condition is reached, the shell temperature increases rapidly, especially in the region immediately behind the nose cap which is in the area of maximum heating.

Comparison With Analysis

Calculations giving the back-surface temperature rises of the Avcoat II and phenolic-nylon models (figs. 5(b) and 5(e)) were made by using the numerical analysis of reference 6. These two models were considered since they represented the two types of materials tested - that is, subliming and char-forming materials. The results from the Avcoat II model were used rather than those for the Teflon model because radiant-heat transfer through the Teflon is not compatible with the model used in the analysis. The phenolic-nylon results were used because phenolic nylon produces a carbonaceous char and the material properties of phenolic nylon are more well known than those of cork.

The analysis was performed for conditions corresponding to those existing at the location of thermocouples 2 and 5. At these locations a heating rate of 45 Btu/(sq ft)(sec) (51×10^4 W/m^2) was used. A comparison between experimental and calculated temperature histories is shown in figures 5(b) and 5(e). The material property values used in the calculations were obtained from available data and are given in table III. However, since little data are available on the specific heat of the gases of pyrolysis and the thermal conductivity of the charred material, particularly at elevated temperatures, the values for these two properties were assumed and varied within reasonable limits to obtain agreement between calculated and experimental results.

As can be seen from figure 5(b), the measured and calculated temperature histories agree closely for the Avcoat II model. The agreement for the phenolic-nylon model (fig. 5(e)) is not as close, in that the calculated temperatures increase faster than the measured temperatures. This lack of agreement might be the result of separation at the bond layer mentioned previously. Another cause of disagreement between calculated and measured temperatures is the two-dimensional heat flow in the model which would reduce the temperature of the magnesium shell at the location chosen for comparison.

CONCLUDING REMARKS

Cone-shaped models, consisting of a truncated magnesium-alloy shell and a contoured plastic nose cap with various thermal protection materials bonded to the magnesium shell, were tested in the 2500-kilowatt arc jet at the Langley Research Center. Measurements of radio-frequency attenuation due to thermal degradation of the protective material were made.

The radio-frequency attenuation measurements indicate that, at least for the test frequency, thermal-protection materials which form appreciable thicknesses of carbonaceous char or electrically conducting debris layers during thermal degradation will not permit satisfactory transmission. Satisfactory transmission can be obtained by inserting antenna windows in otherwise unacceptable protection materials. However, unless the antenna window ablates at the same rate as does the protection material, serious notch effects can develop at the antenna location and can lead to high local heating. From the test results, it appears that materials which sublime when highly heated will permit satisfactory radio-frequency transmission, provided that the material is acceptable before exposure to heating.

The thermal-protection effectiveness calculated from tests performed in the arc-jet environment indicate a wide range of values for the various materials tested. However, this effectiveness cannot be taken as a true indication of the performance of these materials in the flight environment but should be considered a comparison of their performance only in the environment in which they were tested.

Of the materials tested, it appears that only Teflon and Avcoat II will meet the criteria established for protection of a flight-vehicle afterbody. These materials permit satisfactory radio-frequency transmission and are able to to accommodate the heat input without severe surface irregularities or defects.

Langley Research Center,
National Aeronautics and Space Administration,
Langley Station, Hampton, Va., May 8, 1964.

APPENDIX

CONVERSION FACTORS

The International System of Units (SI) was adopted by the Eleventh General Conference on Weights and Measures, Paris, October 1960, in Resolution No. 12 (ref. 1). Conversion factors required for units used here are presented in the following table:

Physical quantity	U.S. customary unit	Conversion factor (a)	SI unit
Heat of pyrolysis	Btu/lb	2.324444×10^3	joules/kilogram (J/kg)
Heating rate	Btu/(sq ft)(sec)	1.134893×10^4	watts/(meter)^2 (W/m^2)
Effectiveness	Btu/lb	2.324444×10^3	joules/kilogram (J/kg)
Length	in.	.0254	meters (m)
Pyrolysis rate	lb/(sq ft)(sec)	4.882428	kilograms/(meter)^2-second (kg/m^2-s)
Specific heat	Btu/lb-$^\circ$R	4.184×10^3	joules/kilogram-$^\circ$Kelvin (J/kg-$^\circ$K)
Temperature	$^\circ$F + 459.67	5/9	$^\circ$Kelvin ($^\circ$K)
	$^\circ$R	5/9	$^\circ$Kelvin ($^\circ$K)
Thermal conductivity	Btu/ft-sec-$^\circ$R	6.24×10^3	watts/meter-$^\circ$Kelvin (W/m-$^\circ$K)
Weight distribution	lb/sq ft	4.882428	kilograms/(meter)^2 (kg/m^2)
Mass flow rate	lb/sec	.453592	kilograms/second (kg/s)

[a]Multiply value given in U.S. customary unit by conversion factor to obtain equivalent value in SI unit.

Prefixes to indicate multiples of units used in this paper are:

milli (m)	10^{-3}
centi (c)	10^{-2}
kilo (k)	10^3
mega (M)	10^6

REFERENCES

1. Anon.: International System of Units - Resolution No. 12. NASA TT F-200, 1964.

2. Chapman, Andrew J.: An Experimental Evaluation of Three Types of Thermal Protection Materials at Moderate Heating Rates and High Total Heat Loads. NASA TN D-1814, 1963.

3. Charwat, A. F., Dewey, C. F., Jr., Roos, J. N., and Hitz, J. A.: An Investigation of Separated Flows - Part II: Flow in the Cavity and Heat Transfer. Jour. Aerospace Sci., vol. 28, no. 7, July 1961, pp. 513-528.

4. Chung, Paul M., and Viegas, John R.: Heat Transfer at the Reattachment Zone of Separated Laminar Boundary Layers. NASA TN D-1072, 1961.

5. Carlson, Walter O.: Heat Transfer in Laminar Separated and Wake Flow Regions. 1959 Heat Transfer and Fluid Mechanics Institute (Univ. of California), Stanford Univ. Press, June 1959, pp. 140-155.

6. Swann, Robert T., and Pittman, Claud M.: Numerical Analysis of the Transient Response of Advanced Thermal Protection Systems for Atmospheric Entry. NASA TN D-1370, 1962.

TABLE I.- DESCRIPTION OF TEST SPECIMENS

Test material	Test-material composition	Specific gravity	Test-material thickness in.	Test-material thickness cm	Bond material
Phenolic nylon	50-percent phenolic + 50-percent nylon (by weight)	1.20	0.25	0.635	Epoxy + fillers
Thermo-Lag T-500 EX167	Inorganic subliming salts + phenolic binder	1.28	.25	.635	Self-bonding
Avcoat II	Epoxy + additives	1.01	.25	.635	Self-bonding
RTV-88	Silicone + thixotropic agent	1.46	.25	.635	Self-bonding
Teflon	Tetrafluoroethylene resin	2.20	.25	.635	Silicone + iron oxide fillers Epoxy + fillers
Cork	Cork + phenolic binder	.45	.25	.635	Epoxy + fillers

TABLE II.- TEST RESULTS

Test material	Test time, seconds	Radio-frequency attenuation, decibels (a)	Effectiveness[b] for various shell temperatures, Btu/lb			kJ/kg		
			100° F	300° F	500° F	311° F	422° F	533° F
Teflon	63	2	315	835	985	732	1,941	2,290
Avcoat II	54	2	1,200	1,655	1,780	2,789	3,847	4,138
Avcoat II[c]	56	2	1,165	1,695	1,910	2,708	3,940	4,440
RTV-88	[d]60	5	617			1,434		
Phenolic nylon	101	30 to 35	950	2,530	2,910	2,208	5,881	6,764
Phenolic nylon[c]	[e]88	2	1,240			2,882		
Cork	56	(f)	3,160	4,000	4,240	7,345	9,298	9,856
Thermo-Lag T-500 EX167	[g]157.5	30 to 35	1,000	3,080	2,900	2,324	7,159	6,741
Thermo-Lag T-500 EX167[c]	[e]91	2	1,030			2,394		

[a]Measured at 950 Mc.
[b]Effectiveness calculated for $q = 45$ Btu/(sq ft)(sec) or (51×10^4) W/m^2.
[c]Specimens with Teflon ring antenna window.
[d]Test terminated because of mechanical failure of arc jet.
[e]Test terminated because of undercutting of Teflon ring antenna window.
[f]Severe attenuation; reading not reliable.
[g]Test terminated because of appearance of large craters in test material.

TABLE III.- MATERIAL PROPERTY VALUES

Avcoat II:

Char:

Specific gravity	0.32
Specific heat, Btu/lb-°R (J/kg-°K)	0.43 (1.80×10^3)
Thermal conductivity, Btu/ft-sec-°R (W/m-°K), for -	
500° R (278° K)	2.0×10^{-5} (0.1248)
2,000° R (1111° K)	2.0×10^{-5} (0.1248)
4,000° R (2222° K)	1.0×10^{-4} (0.624)
Emissivity	1.0

Uncharred material:

Specific gravity	1.01
Specific heat, Btu/lb-°R (J/kg-°K)	0.43 (1.8×10^3)
Thermal conductivity, Btu/ft-sec-°R (W/m-°K)	2.5×10^{-5} (0.156)

Miscellaneous:

Specific heat of gaseous products of pyrolysis, Btu/lb-°R (J/kg-°K)	0.3 (1.26×10^3)
Heat of pyrolysis, Btu/lb (J/kg)	250 (581×10^3)
Pyrolysis rate, lb/(sq ft)(sec)	$\left(9.96 \times 10^6\right) \exp\left(\frac{2.763 \times 10^4}{\text{Pyrolysis temperature, } ^\circ R}\right)$
Pyrolysis rate, kg/m^2-sec	$\left(4.86 \times 10^7\right) \exp\left(\frac{1.535 \times 10^4}{\text{Pyrolysis temperature, } ^\circ K}\right)$

Phenolic nylon:

Char:

Specific gravity	0.481
Specific heat, Btu/lb-°R (J/kg-°K)	0.5 (2.09×10^3)
Thermal conductivity, Btu/ft-sec-°R (W/m-°K), for -	
500° R (278° K)	5×10^{-6} (0.0312)
1,000° R (556° K)	1×10^{-5} (0.0624)
1,500° R (833° K)	5×10^{-5} (0.312)
2,000° R (1111° K)	1×10^{-4} (0.624)
4,000° R (2222° K)	1×10^{-3} (6.24)
Emissivity	0.8

Uncharred material:

Specific gravity	1.20
Specific heat, Btu/lb-°R (J/kg-°K)	0.38 (1.59×10^3)
Thermal conductivity, Btu/ft-sec-°R (W/m-°K)	2×10^{-5} (0.1248)

Miscellaneous:

Specific heat of gaseous products of pyrolysis, Btu/lb-°R (J/kg-°K), for -	
500° R (278° K)	0.3 (1.26×10^3)
1,000° R (556° K)	0.45 (1.88×10^3)
2,000° R (1111° K)	0.7 (2.92×10^3)
4,000° R (2222° K)	1.0 (4.18×10^3)
Heat of pyrolysis, Btu/lb (J/kg)	230 (535×10^3)
Pyrolysis rate, lb/(sq ft)(sec)	$\left(1.0 \times 10^7\right) \exp\left(\frac{2.763 \times 10^4}{\text{Pyrolysis temperature, } ^\circ R}\right)$
Pyrolysis rate, kg/m^2-sec	$\left(4.88 \times 10^7\right) \exp\left(\frac{1.535 \times 10^4}{\text{Pyrolysis temperature, } ^\circ K}\right)$

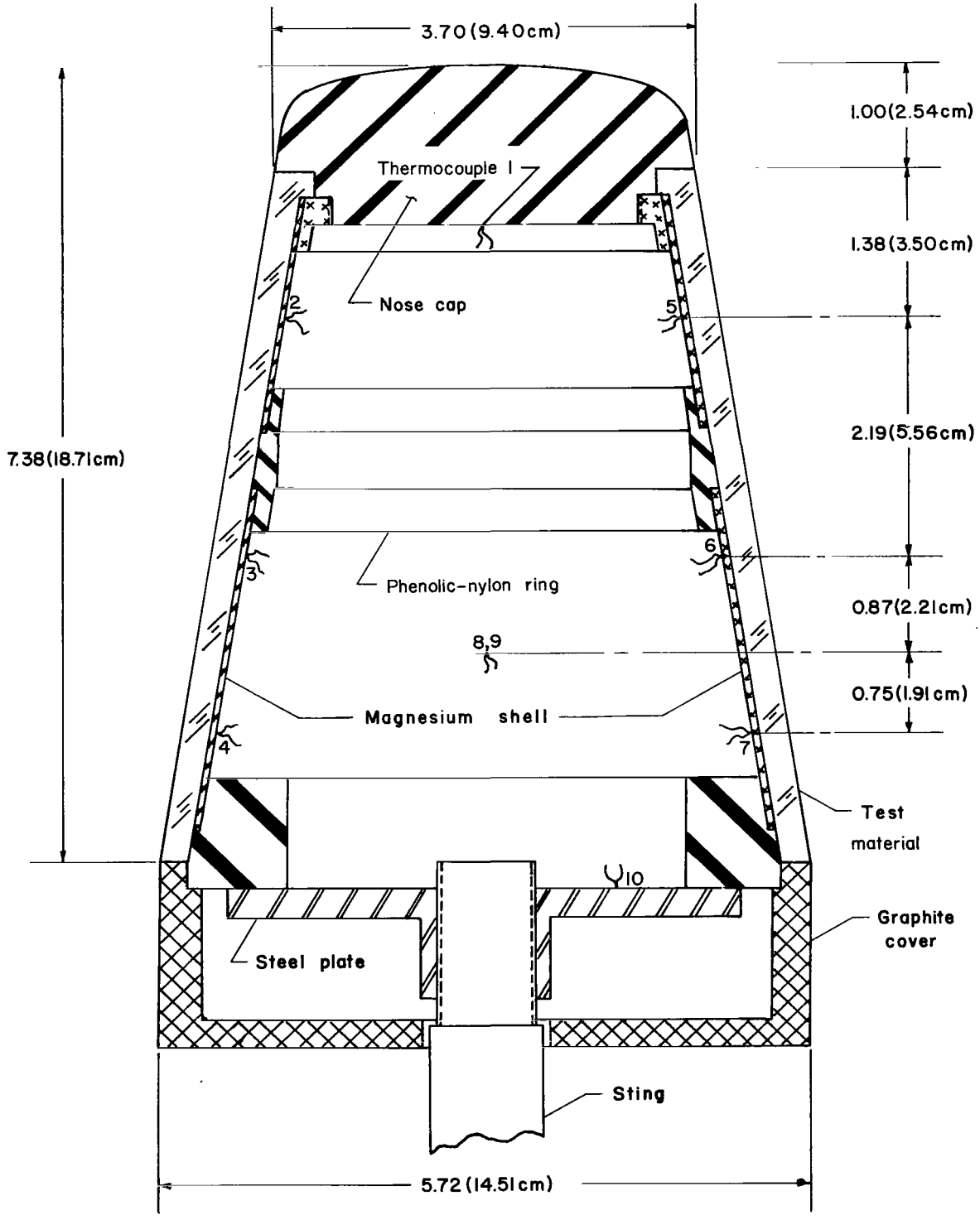

Figure 1.- Model configuration showing thermocouple location.

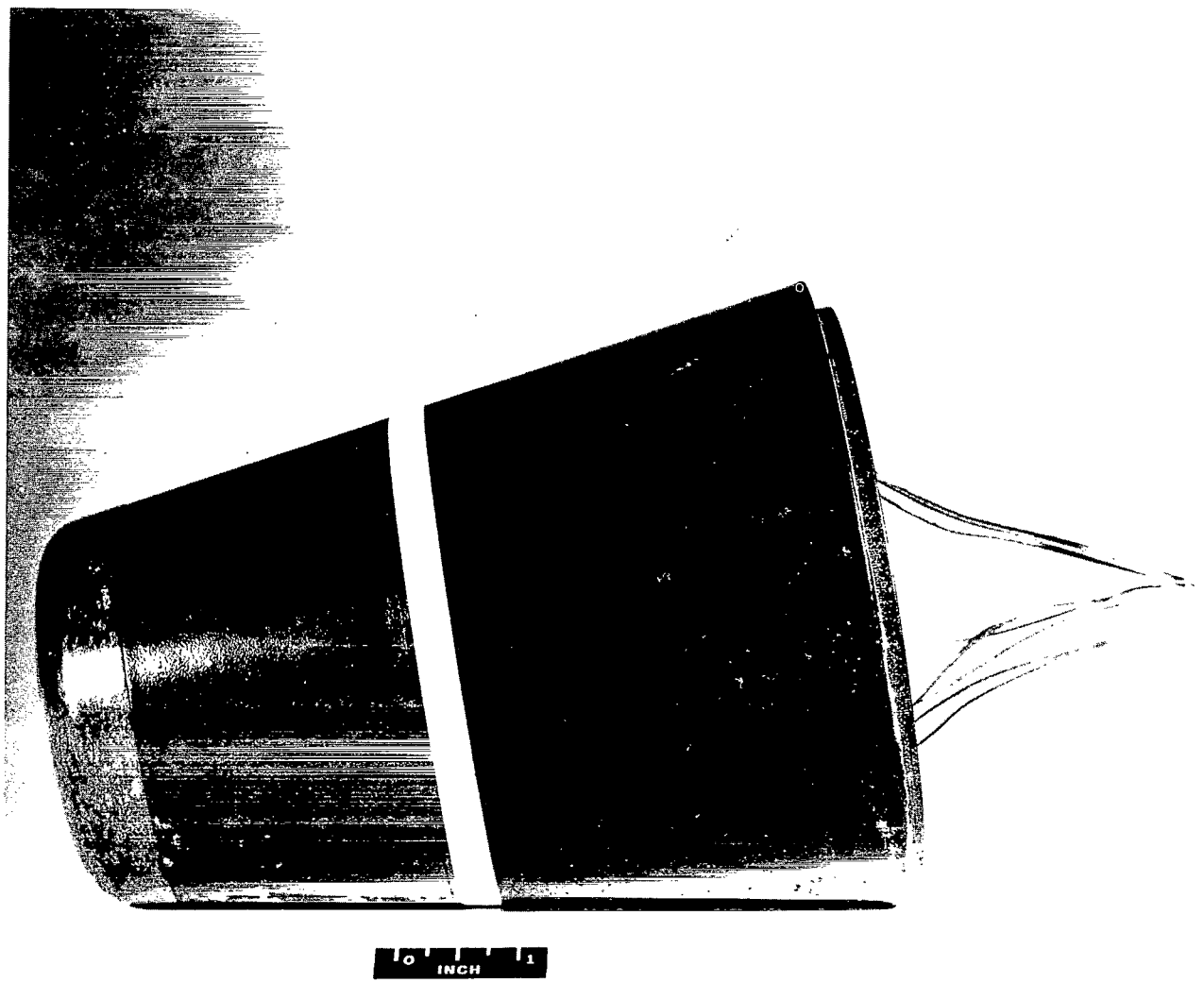

(a) Thermo-Lag T-500 EX167 model with Teflon ring antenna. L-61-6577

Figure 2.- Typical models.

(b) RTV-88 model without Teflon ring antenna. L-61-8000

Figure 2.- Concluded.

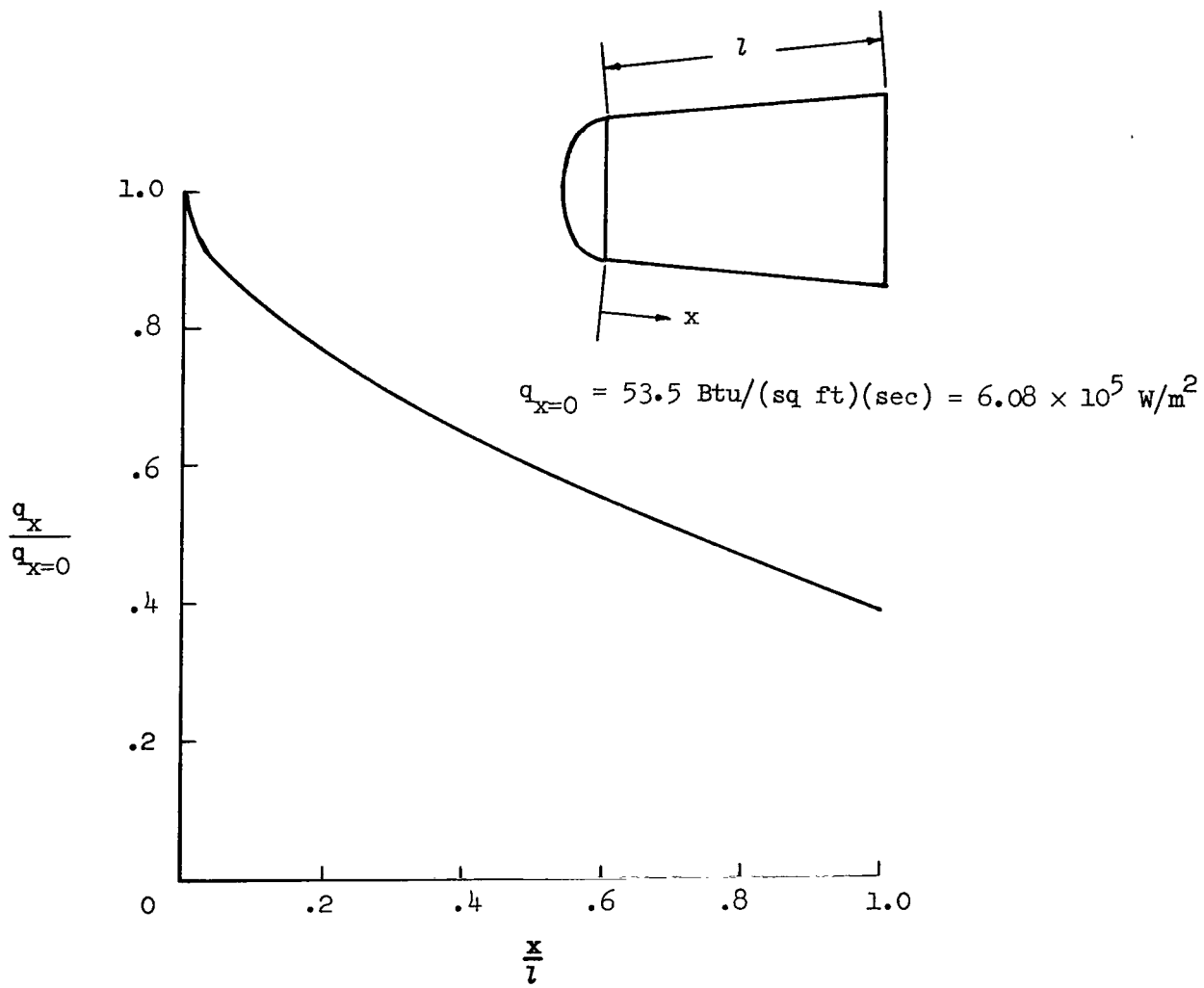

Figure 3.- Measured afterbody cold-wall heating-rate distributions.

Figure 4.- Test setup. L-61-6822.1

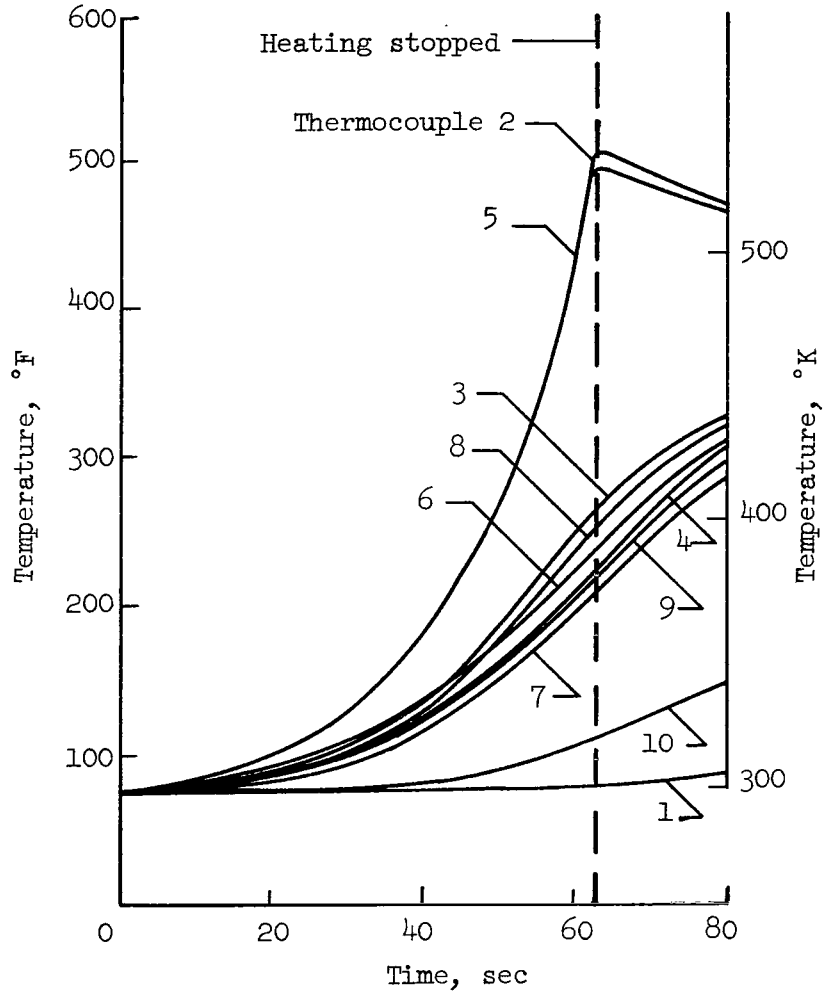

(a) Teflon.

Figure 5.- Temperature histories.

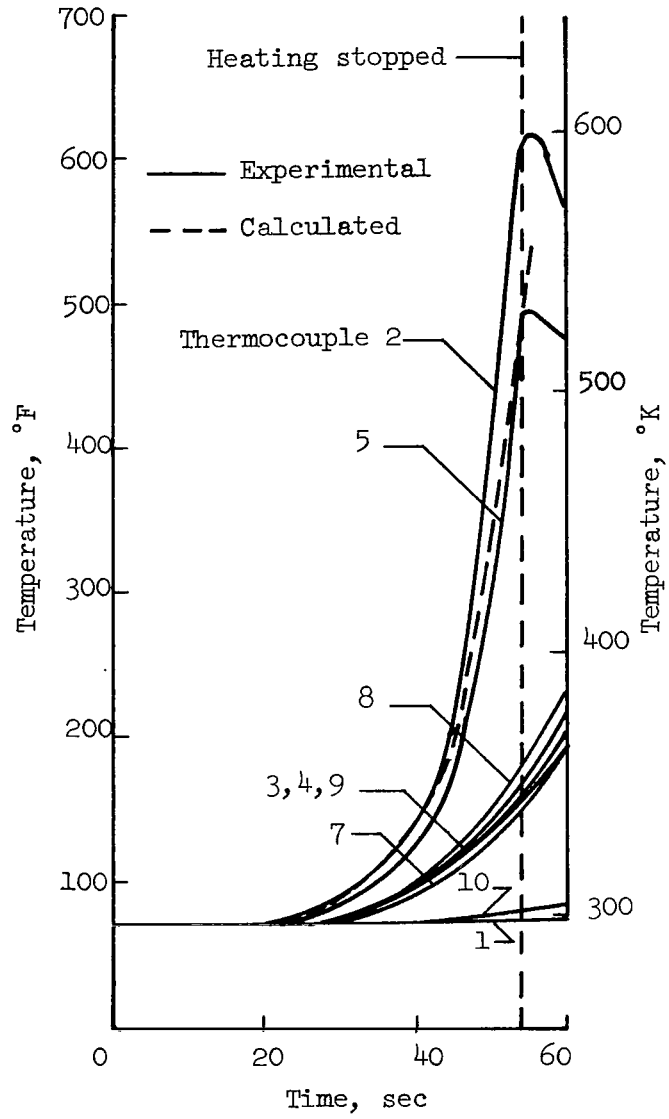

(b) Avcoat II.

Figure 5.- Continued.

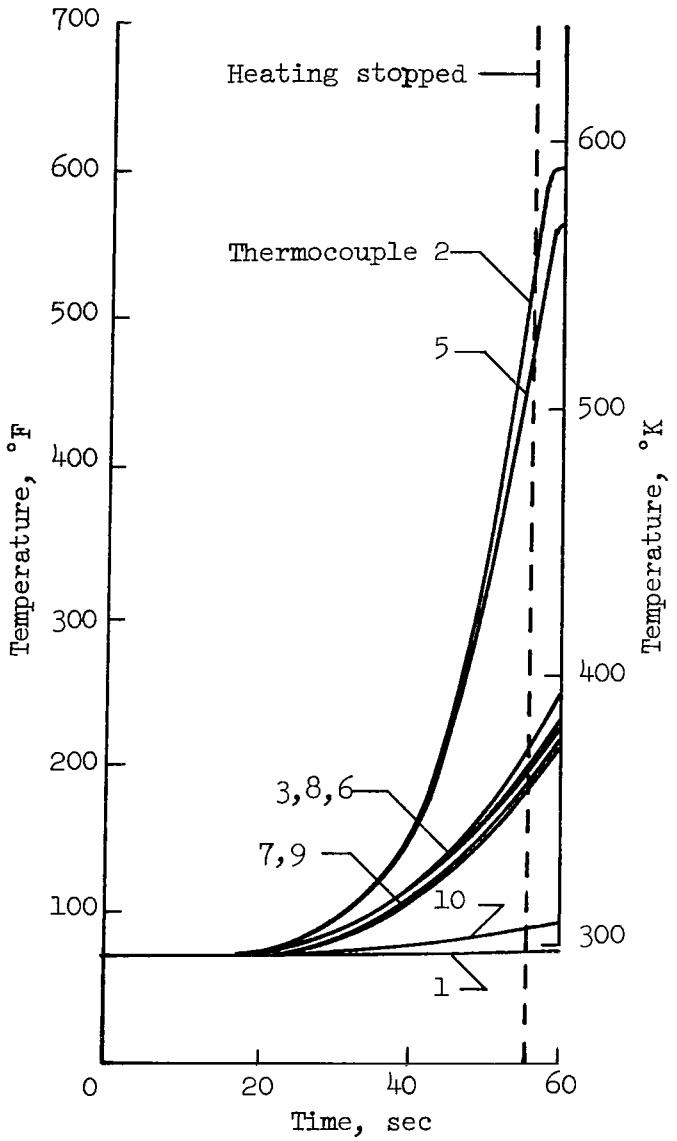

(c) Avcoat II with Teflon ring.

Figure 5.- Continued.

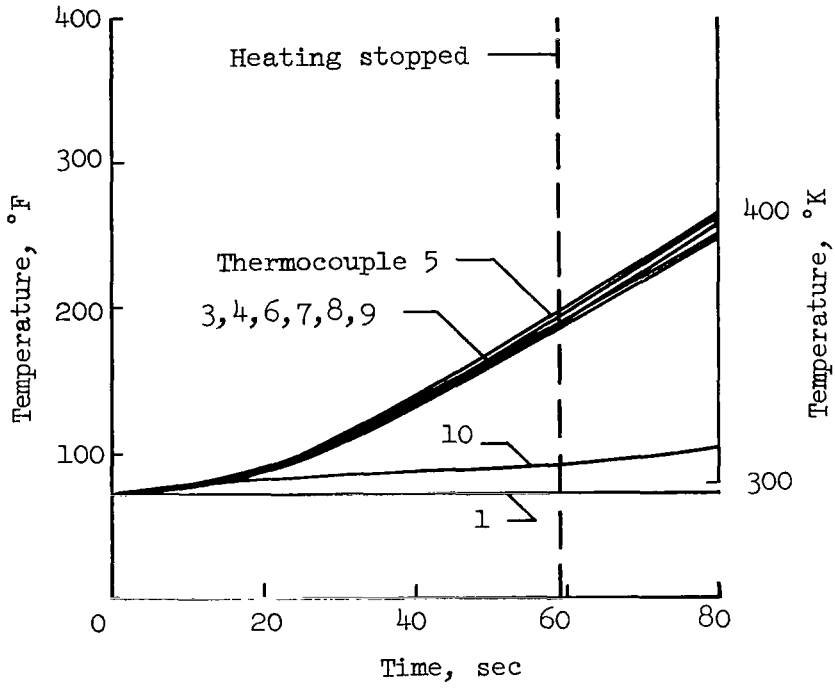

(d) RTV-88.

Figure 5.- Continued.

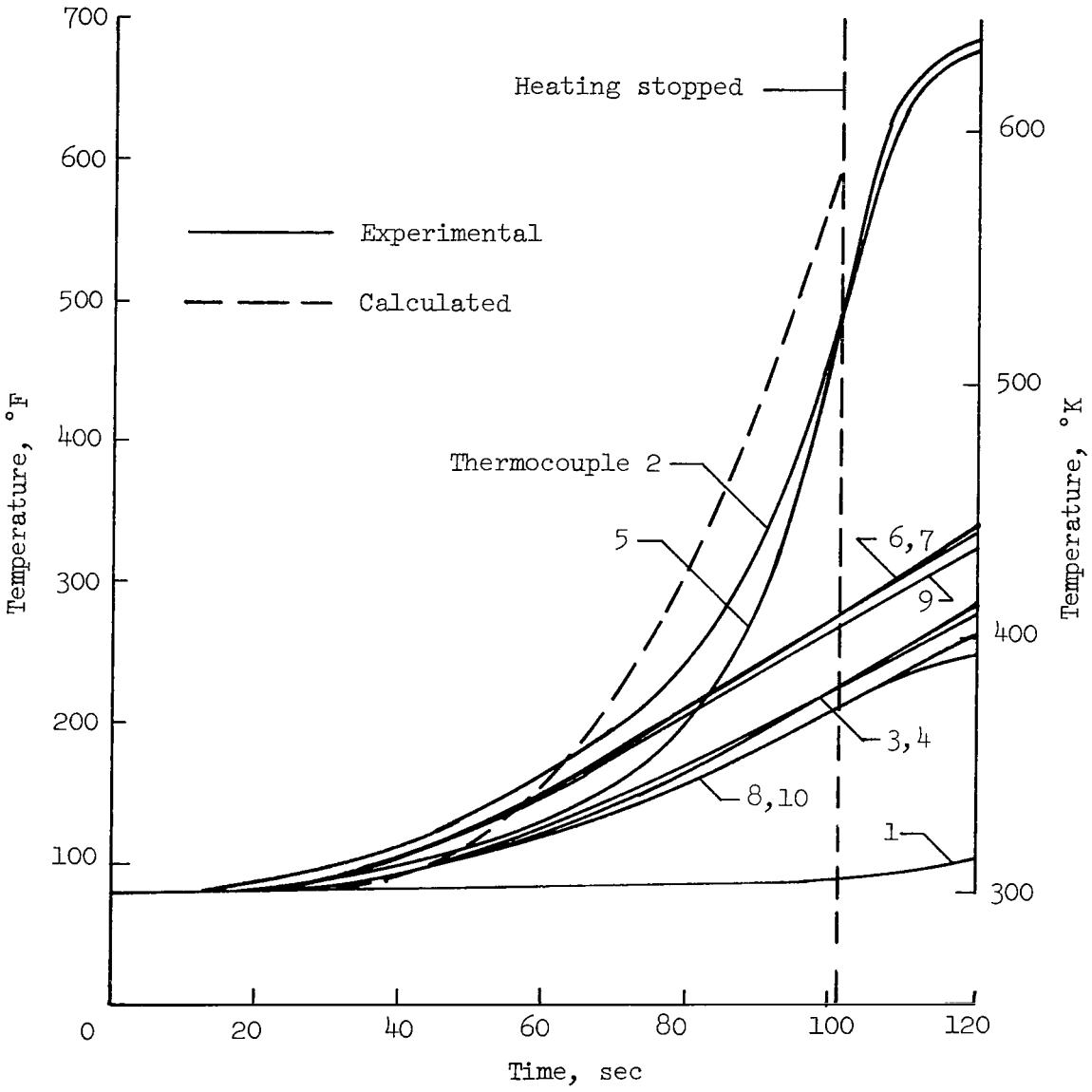

(e) Phenolic nylon.

Figure 5.- Continued.

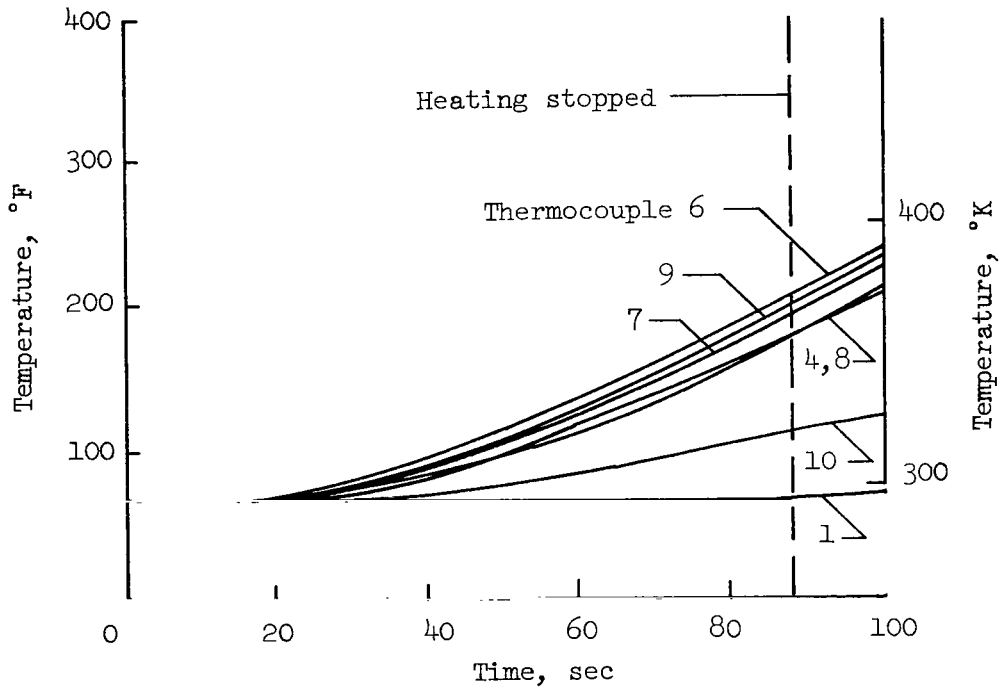

(f) Phenolic nylon with Teflon ring.

Figure 5.- Continued.

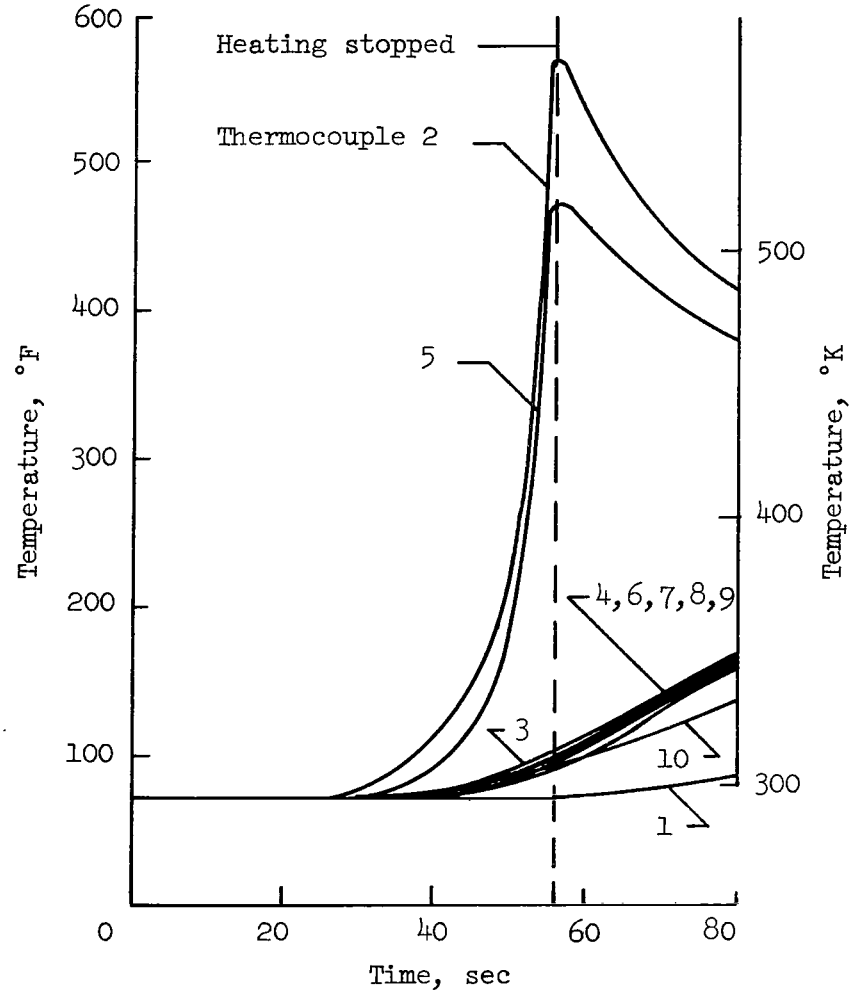

(g) Cork.

Figure 5.- Continued.

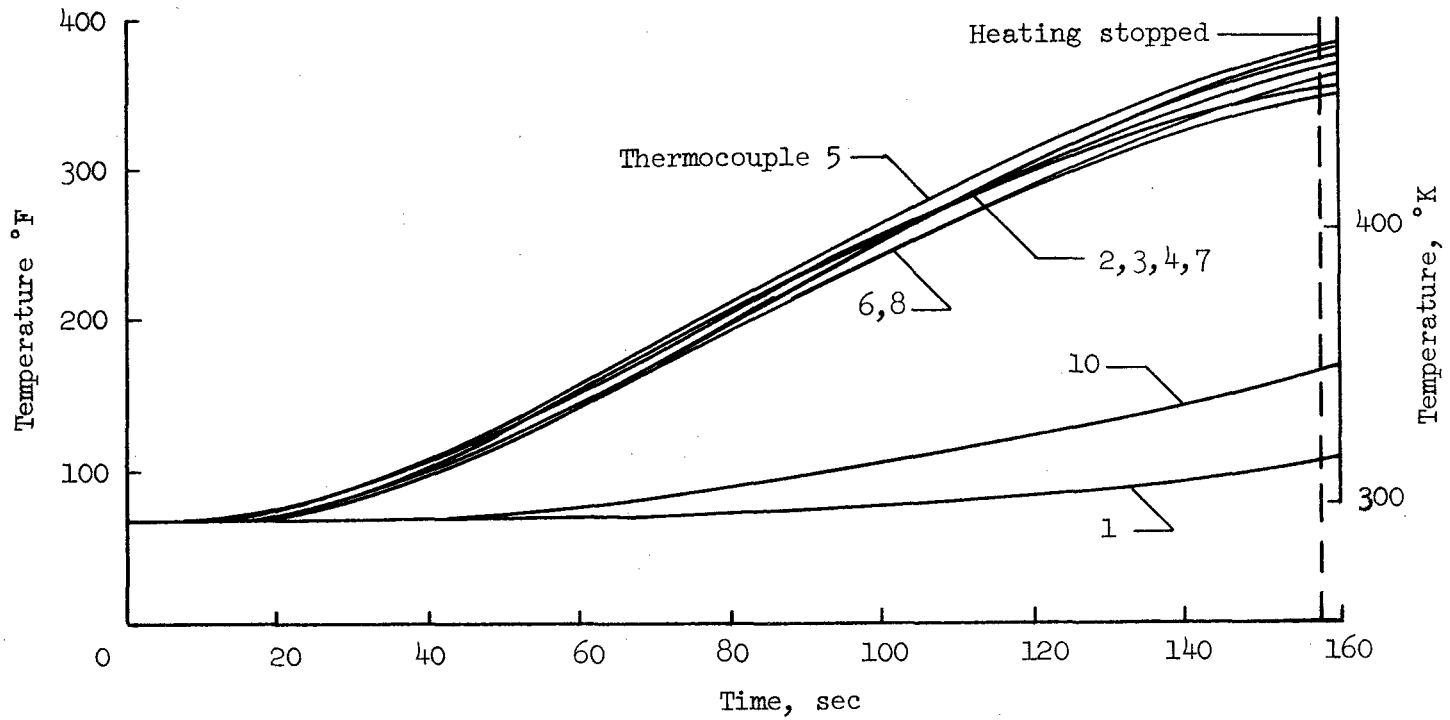

(h) Thermo-Lag T-500 EX167.

Figure 5.- Continued.

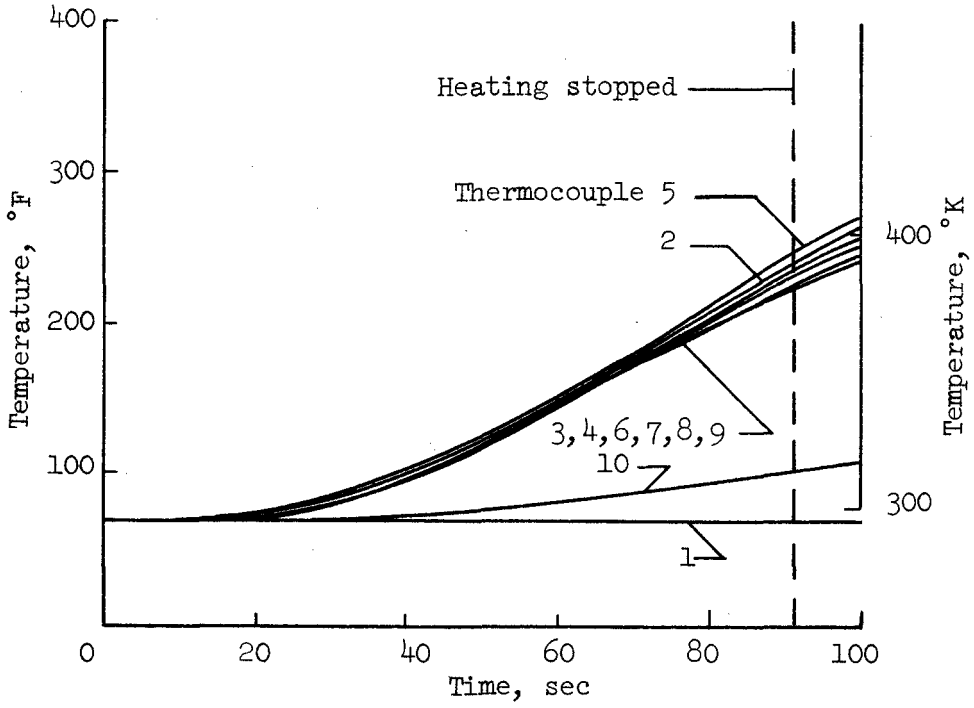

(i) Thermo-Lag T-500 EX167 with Teflon ring.

Figure 5.- Concluded.

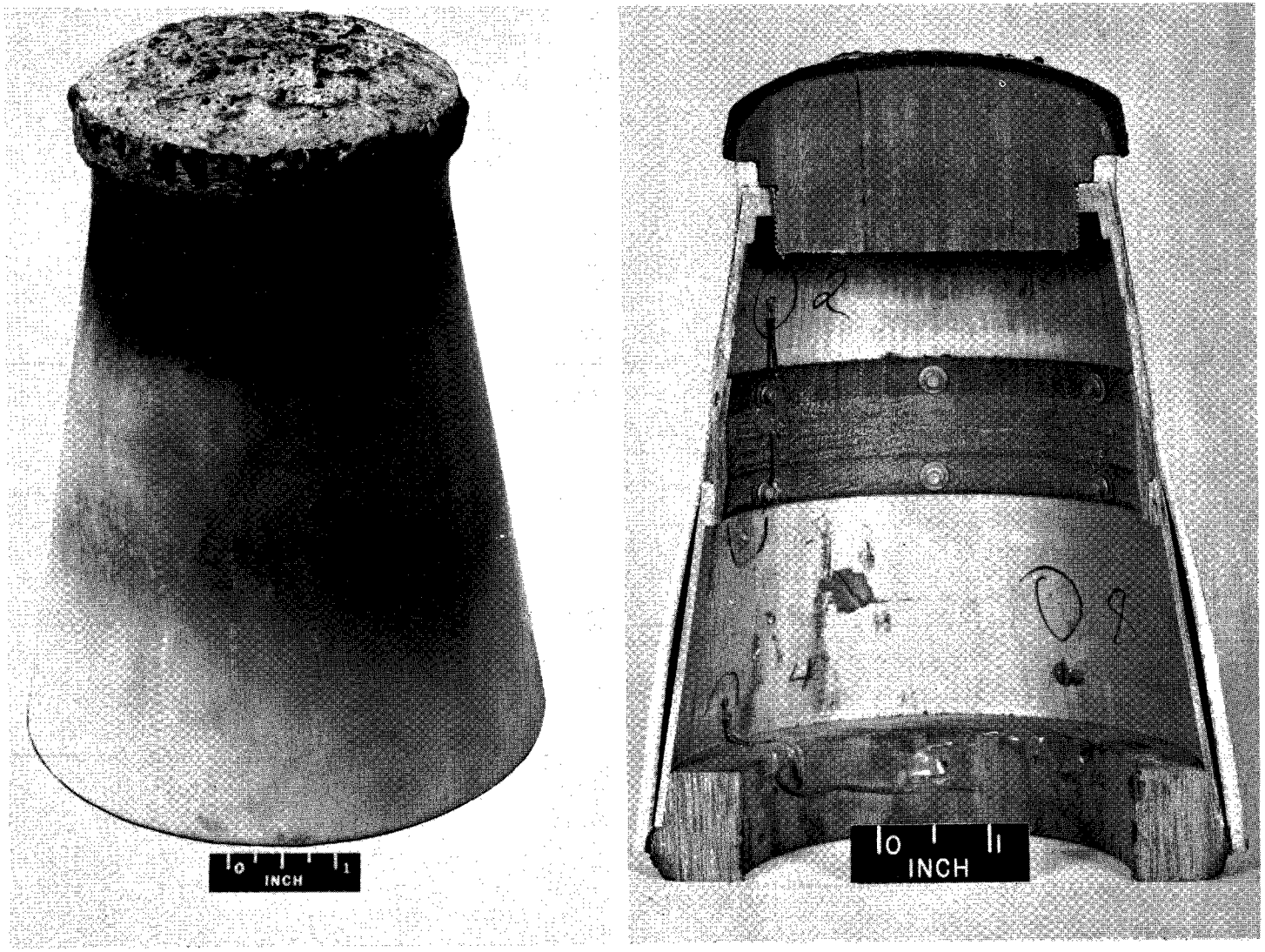

L-62-3679 L-63-7386

(a) Teflon.

Figure 6.- Models after testing.

L-61-6820

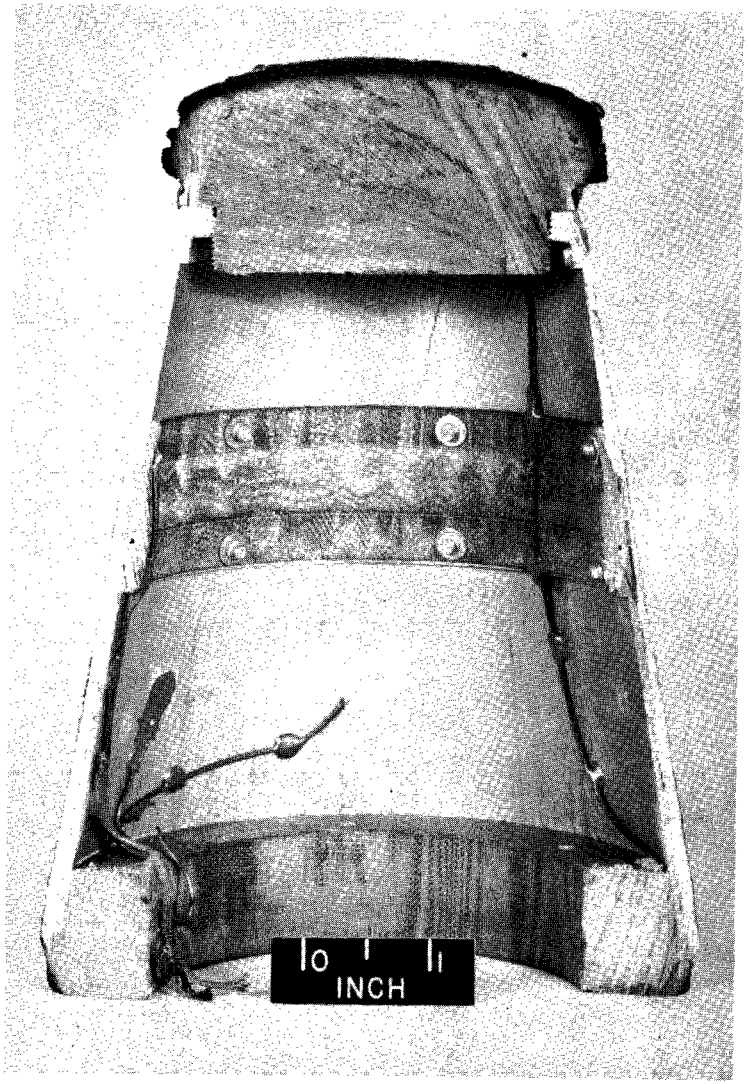

L-63-7385

(b) Avcoat II.

Figure 6.- Continued.

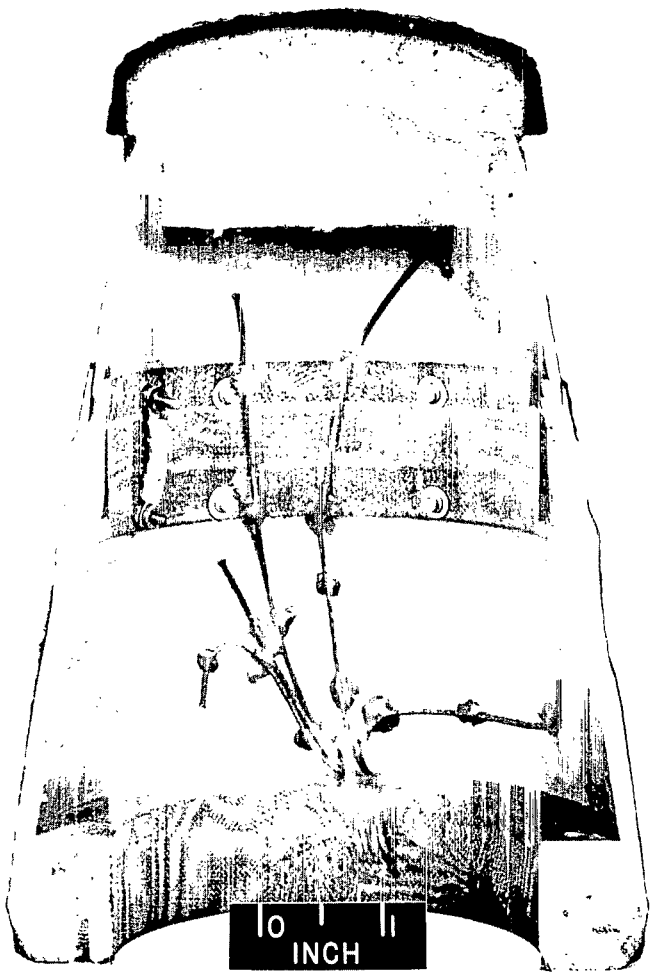

L-61-6821

L-63-7384

(c) Avcoat II with Teflon ring antenna window.

Figure 6.- Continued.

L-62-3678

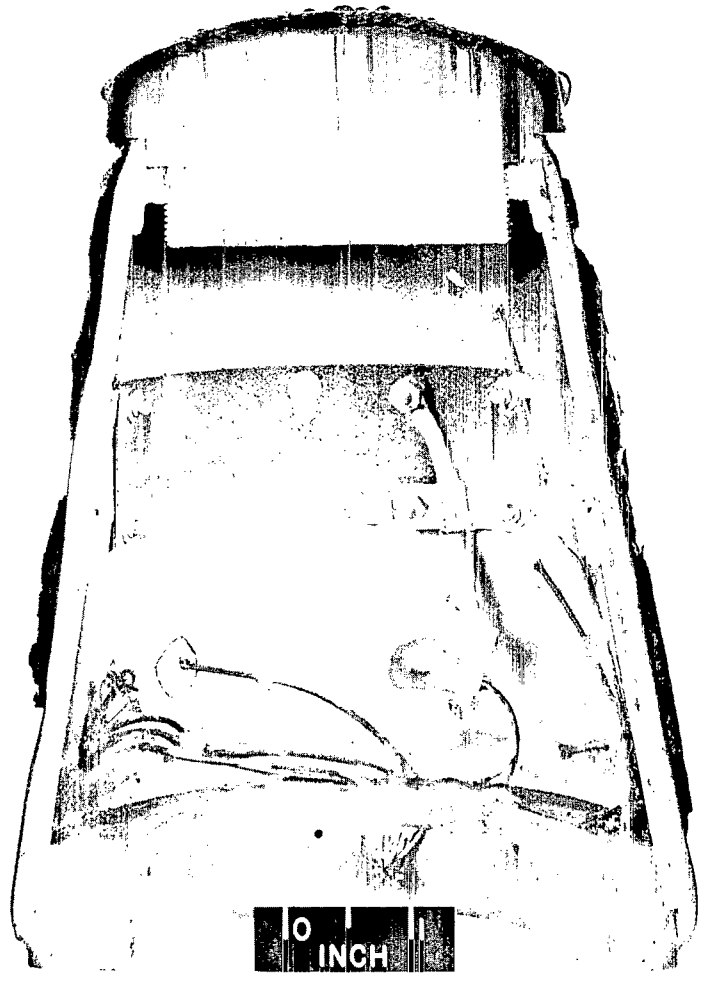

L-63-7380

(d) RTV-88.

Figure 6.- Continued.

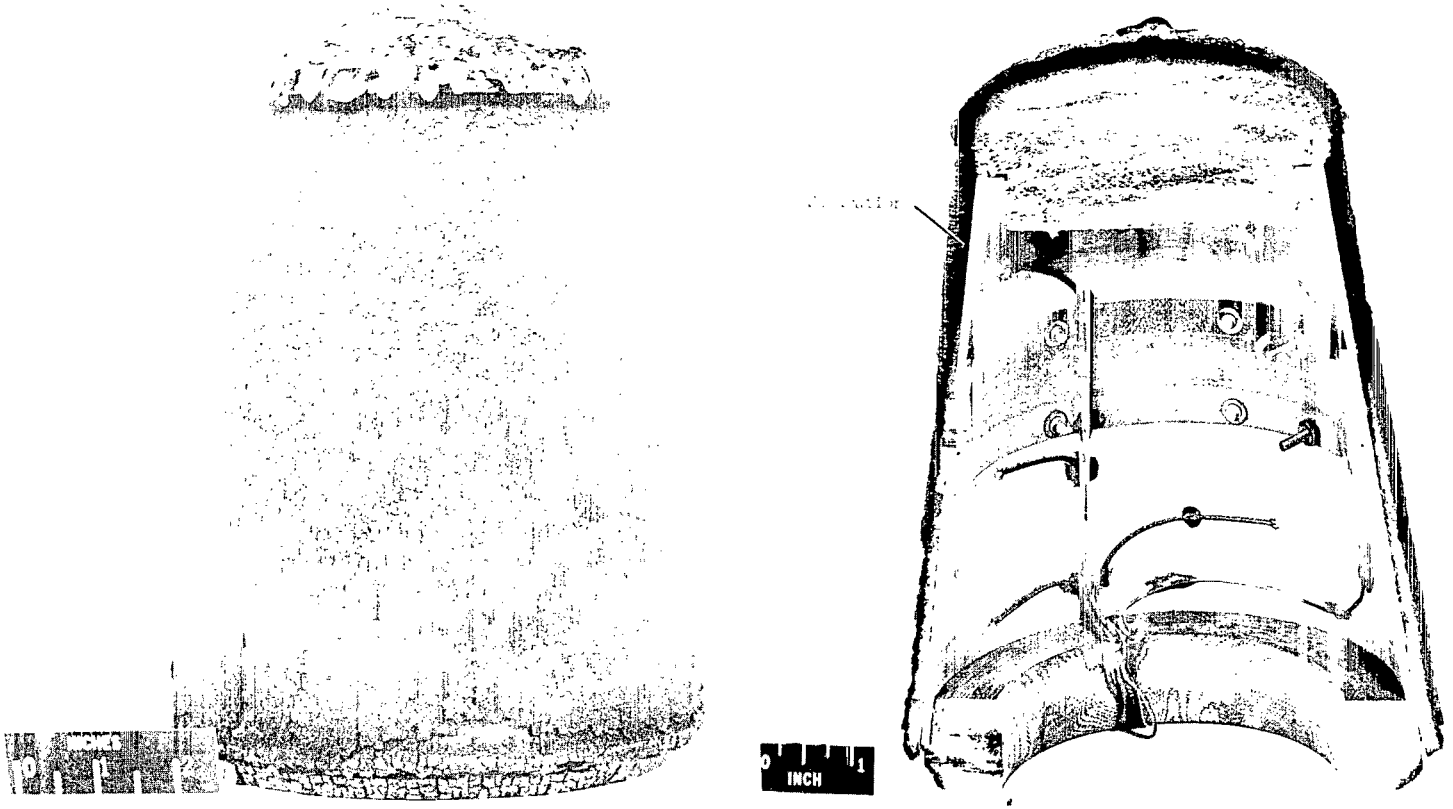

(e) Phenolic nylon. L-64-3100

Figure 6.- Continued.

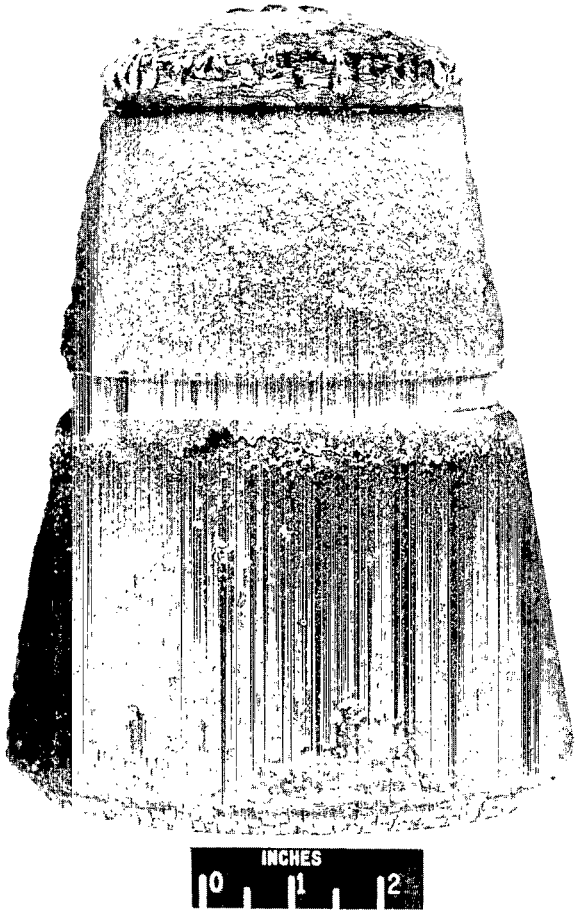

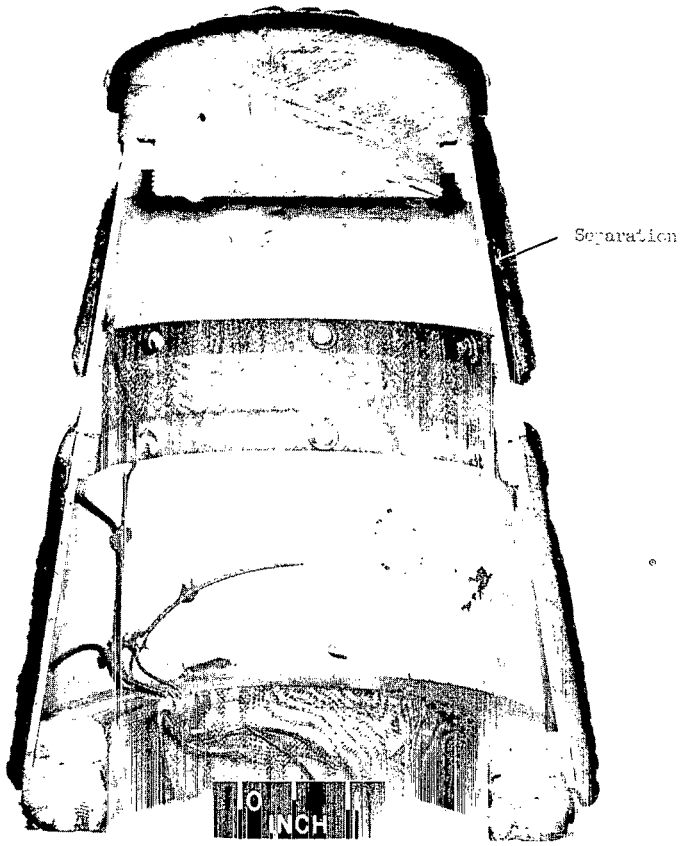

L-64-4701

(f) Phenolic nylon with Teflon ring antenna window.

Figure 6.- Continued.

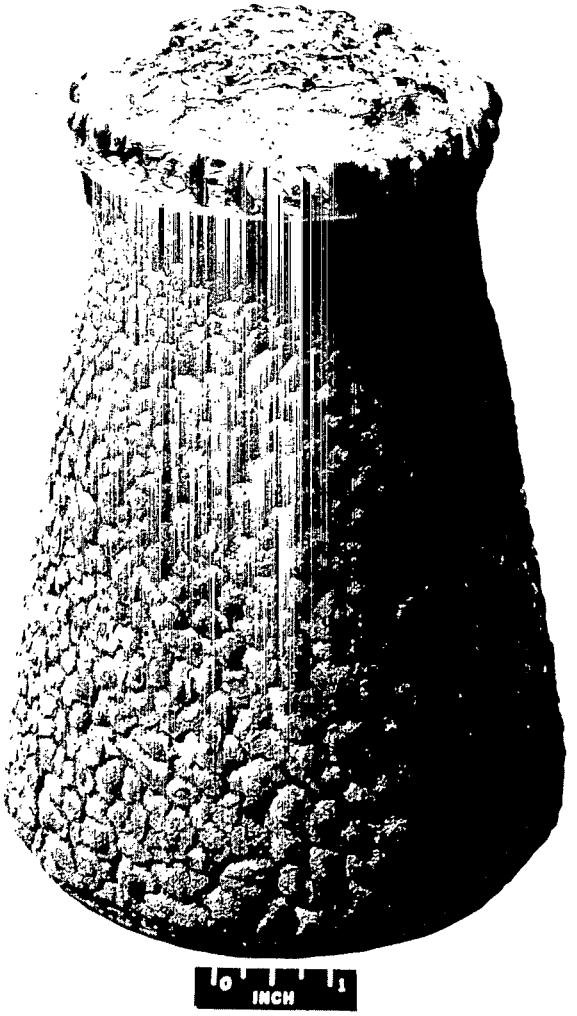

L-62-3677

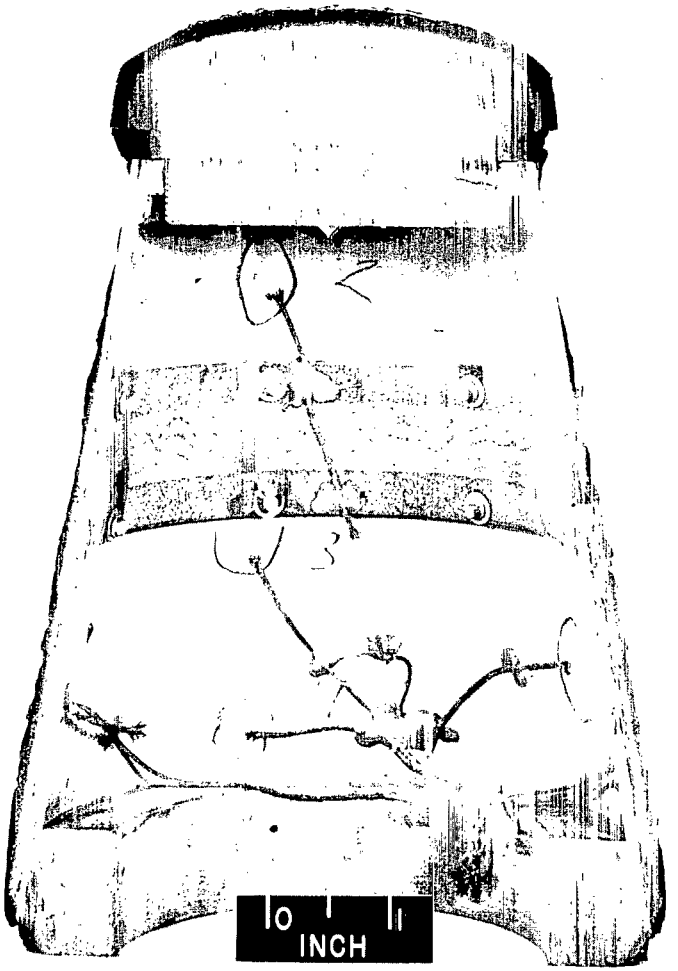

L-63-7383

(g) Cork.

Figure 6.- Continued.

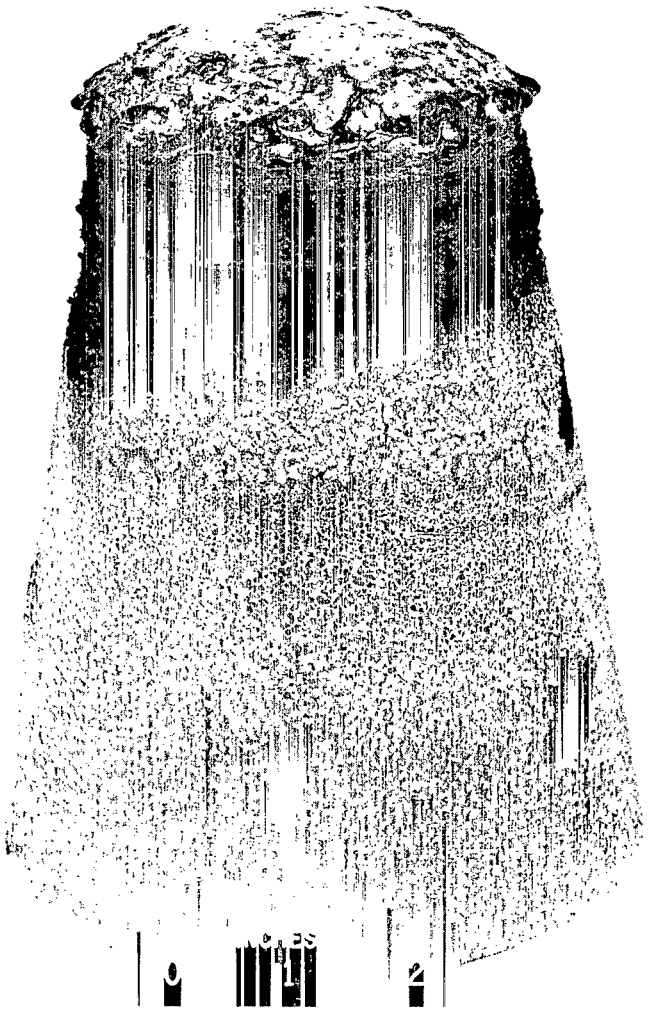

L-61-6818

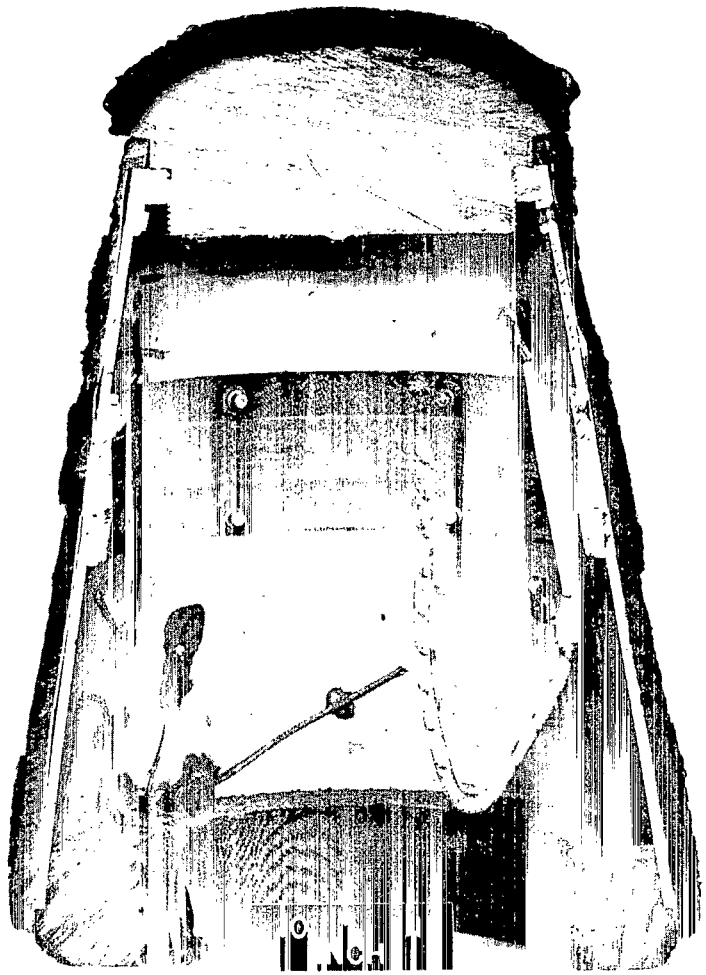

L-63-7381

(h) Thermo-Lag T-500 EX167.

Figure 6.- Continued.

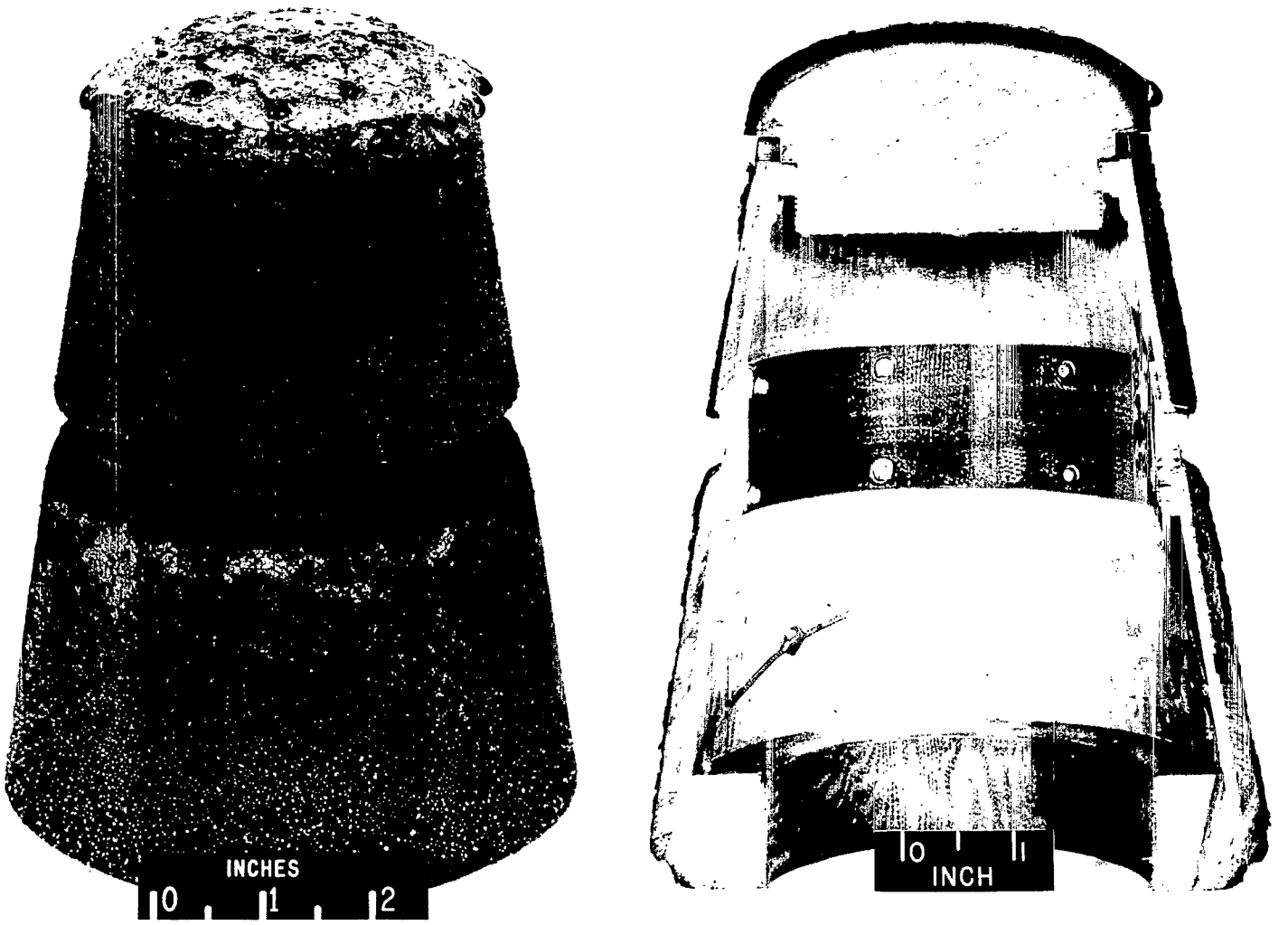

L-61-6819 L-63-7379

(i) Thermo-Lag T-500 EX167 with Teflon ring antenna window.

Figure 6.- Concluded.

"The aeronautical and space activities of the United States shall be conducted so as to contribute . . . to the expansion of human knowledge of phenomena in the atmosphere and space. The Administration shall provide for the widest practicable and appropriate dissemination of information concerning its activities and the results thereof."

—NATIONAL AERONAUTICS AND SPACE ACT OF 1958

NASA SCIENTIFIC AND TECHNICAL PUBLICATIONS

TECHNICAL REPORTS: Scientific and technical information considered important, complete, and a lasting contribution to existing knowledge.

TECHNICAL NOTES: Information less broad in scope but nevertheless of importance as a contribution to existing knowledge.

TECHNICAL MEMORANDUMS: Information receiving limited distribution because of preliminary data, security classification, or other reasons.

CONTRACTOR REPORTS: Technical information generated in connection with a NASA contract or grant and released under NASA auspices.

TECHNICAL TRANSLATIONS: Information published in a foreign language considered to merit NASA distribution in English.

TECHNICAL REPRINTS: Information derived from NASA activities and initially published in the form of journal articles.

SPECIAL PUBLICATIONS: Information derived from or of value to NASA activities but not necessarily reporting the results of individual NASA-programmed scientific efforts. Publications include conference proceedings, monographs, data compilations, handbooks, sourcebooks, and special bibliographies.

Details on the availability of these publications may be obtained from:

SCIENTIFIC AND TECHNICAL INFORMATION DIVISION

NATIONAL AERONAUTICS AND SPACE ADMINISTRATION

Washington, D.C. 20546